HHS Public Access

Author manuscript

Magn Reson Med. Author manuscript; available in PMC 2017 September 01.

Published in final edited form as:

Magn Reson Med. 2016 September ; 76(3): 1007–1014. doi:10.1002/mrm.26002.

Low-temperature dynamic nuclear polarization of gases in frozen mixtures

Mehrdad Pourfathi[1,2], **Justin Clapp**[1], **Stephen J. Kadlecek**[1], **Caroline D. Keenan**[1], **Rajat K. Ghosh**[1], **Nicholas N. Kuzma**[1], and **Rahim R. Rizi**[1,*]

[1]Department of Radiology, University of Pennsylvania, Philadelphia, PA 19104, United States

[2]Department of Electrical and Systems Engineering, University of Pennsylvania, PA 19104, United States

Abstract

Purpose—To present a new cryogenic technique for preparing gaseous compounds in solid mixtures for polarization using dynamic nuclear polarization (DNP).

Methods—^{129}Xe and $^{15}N_2O$ samples were prepared using the presented method. Samples were hyperpolarized at 1.42K at 5T. ^{129}Xe was polarized at 1.65K and 1.42K to compare enhancement. Polarization levels for both samples and T_1 relaxation times for the ^{129}Xe sample were measured. Sample pulverization for the ^{129}Xe and controlled annealing for both samples were introduced as additional steps in sample preparation.

Results—Enhancement increased by 15% due to a temperature drop from 1.65K to 1.42K for the ^{129}Xe sample. A polarization level of 20±3% for the ^{129}Xe sample was achieved, a 2-fold increase from 10±1% after pulverization of the sample at 1.42K. T_1 of the ^{129}Xe sample was increased by more than 3-fold via annealing. In the case of $^{15}N_2O$, annealing led to a ~2-fold increase in the signal level after DNP.

Conclusion—The presented technique for producing and manipulating solid gas/glassing agent/radical mixtures for DNP led to high polarization levels in ^{129}Xe and $^{15}N_2O$ samples. These methods show potential for polarizing other gases using DNP technology.

Keywords

Hyperpolarization; Dynamic Nuclear Polarization; Gas MRI; Sample Preparation

INTRODUCTION

Hyperpolarized (HP) gas magnetic resonance imaging (MRI) research has generated innovative methods for measuring regional parameters of pulmonary function and structure (1,2). The expansion of this approach relies on the development of a polarization technique that can be feasibly implemented at diverse sites to efficiently produce a range of highly polarized gases. Dynamic nuclear polarization (DNP) offers a promising means of achieving

Corresponding Authors: Rahim R. Rizi, University of Pennsylvania, Department of Radiology, 3450 Hamilton Walk, 308B Stemmler Hall, Philadelphia, PA 19104, United States, Tel: 215-573-0891, rizi@uphs.upenn.edu.

these goals. In contrast to the optical pumping technology traditionally used to hyperpolarize gases, DNP facilities are becoming increasingly available at numerous institutions due to their central role in liquid HP MR. Furthermore, DNP offers the potential to polarize molecular gases, which cannot currently be polarized at a practical scale using other methods—a limitation that has so far constrained HP gas MRI to just two noble gases (^{3}He and ^{129}Xe). Recent reports (3-6) on the DNP of ^{129}Xe suggest that polarization levels generated via DNP are comparable to those typical of optical pumping (3,7-9), and since solid-state DNP is performed at densities much greater than the gas phase, it can potentially produce a larger quantity of hyperpolarized gas than is practical using optical pumping (4,10,11). Motivated by the many potential advantages of gas DNP, this study implements a method for preparing polarized samples that are highly amenable to hyperpolarization using this technology.

We first address a fundamental challenge of polarizing gaseous targets via DNP: proper microscopic mixing of the target, unpaired electron source (e.g., trityl radical (12-14)), and crystallization-preventing glassing agent. Minor deviations in sample preparation can produce heterogeneous samples with very poor polarization characteristics. As with all DNP samples, the components must be vigorously-mixed while in the liquid phase, but the characteristically high vapor pressures of the gas phase nuclei compared to the polar solvents used as glassing agents make this process very difficult. The custom-made gas manifold apparatus we describe below is designed to allow for tight regulation of the temperature and pressure in the manifold in order to ensure that the components remain in the same phase.

Next, we seek to quantify the effect of lowering sample temperature on DNP polarization level. While it is well established that lowering the temperature of the solid-state mixture increases polarization (15-17), the efficiency of the vacuum pump in the DNP unit sets a hard limit on the minimum temperature of the system (4,15). Nevertheless, through optimizing adjustment of the liquid helium level, we attempt to ensure that polarization occurs at the lowest temperature possible within this constraint.

Finally, we describe two additional techniques that can be implemented to enhance the polarization of DNP gases: (1) sample pulverization, which increases thermal contact between the solid-state sample and the helium bath; and (2) controlled annealing, which reintroduces inhomogeneity into the mixture on a microscopic scale by forming clusters of pure gas inside the homogeneous matrix. Pulverization and annealing have previously been shown to preserve overall sample composition while not only elevating polarization level but also lengthening T_1 relaxation time (4,11,18). The latter is of vital importance when considering the practicality of transporting the polarized sample for eventual use in imaging studies. In this paper, we broaden our exploration of these additional steps, addressing the conditions under which these techniques facilitate better polarization and transport and the extent of the benefits that can be expected from them.

We chose here to apply our DNP approach to ^{129}Xe and doubly labeled $^{15}N_2O$, as each of these agents shows significant potential for use in clinical HP MRI research. ^{129}Xe has recently been utilized in human studies to measure ventilation, oxygen tension, and diffusion in a more cost-effective manner than ^{3}He, and it has the capacity to examine gas exchange in

a novel manner due to its solubility in blood and tissue (1,10,19,20). Doubly labeled $^{15}N_2O$ has attracted interest because of its ability to store nuclear polarization when in a long-lived singlet state (21-24). Such states offer the possibility of imaging slower metabolic processes or bio-distribution at quasi-equilibrium; they also may assist with the transport of hyperpolarized biomarkers to clinical sites before polarization is lost, a task that currently poses a major limitation for the clinical application of DNP (12,21). Another potential imaging application for $^{15}N_2O$ measuring the cerebral blood flow (25). While this paper focuses specifically on DNP of ^{129}Xe and $^{15}N_2O$, it is important to note that the methods we have developed are applicable to any gaseous system of interest as a hyperpolarized biomarker so long as it can be mixed with a radical and glassing agent in liquid form.

METHODS

Figure 1 schematically represents the experimental methods we implemented here for the polarization of gaseous samples. In this section, we first describe the construction of the sample mixing manifold and a 5T DNP system. Two distinct approaches for enhancing polarization level and the T_1 relaxation time of the polarized sample are then presented: pulverization and annealing.

Sample Mixing

Samples were prepared using a custom-built gas manifold equipped with a hermitically sealed magnetic stirrer. Samples were composed of trityl (Finland acid) radical, 1-propanol, and liquid gas (3:1 by volume). The liquid gases utilized were ^{129}Xe (natural, BOC Gases, 99.997% purity, <1 ppm O_2 *or* enriched, Linde, 86% enriched, 99% pure) or doubly labeled $^{15}N_2O$ (Cambridge Isotopes, >98% enriched, >98% pure).

Figure 2 shows a basic 3-step schematic of the system that was used to produce solid gaseous mixtures. In **step 1** (Figure 2.1), a mixture of 97 mg of 1-propanol and 3 mg of trityl radical (Finland acid) was prepared in a 5mm sample NMR tube **(A)** and subsequently attached to the hermitically sealed manifold and two small magnetic stir bars **(B)** were placed inside the mixture. The tube was then attached to the manifold and was evacuated to <0.1 mbar. Next, the syringe **(D)** was filled with the target gas by opening valve **(C)**. The volume of the gas used in the mixture was measured by syringe, after adding in the 1.5 ml dead volume of the tubing between valves **(C)**, **(F)** and the syringe. After the desired volume was introduced (20 mL at STP in this study for all samples), valve **(C)** was closed.

In **step 2** (Figure 2.2), the pressure of the target gas was adjusted by increasing or decreasing the pressure inside the sealed vessel **(E)** containing the syringe. This adjustment was accomplished by opening valve **(G)** to let pressurizing gas (nitrogen or air) in or opening valve **(G)** to depressurize the chamber. The pressure was monitored by the pressure gauge **(I)** and increased to the target pressure P_1 (1.75 atm and 4.2 atm for $^{15}N_2O$ and ^{129}Xe, respectively). Then, the 5mm NMR tube containing the mixture was immersed in the liquefaction bath (ethanol/dry-ice) **(J)** at 195 K to liquefy the gas while keeping the 1-propanol/radical mixture in the liquid phase. Once the mixture had equilibrated, valve **(F)** was opened. As the target gas volume (typically ~20 ml) was cryo-pumped into the NMR tube and mixed with the radical solution, a magnetic stirrer **(K)** was used to spin the small

magnetic stir bars **(B)** inside the sample mixture for 1 minute to achieve a homogeneous mixture

In **step 3** (Figure 2.3), the small magnetic stir bars were removed from the mixture using an external magnet **(K)**, and the liquefaction bath was then quickly swapped with liquid nitrogen **(L)** to solidify the mixture. Frozen pure gas on top of the mixture inside the sample test tube was occasionally deposited. A warm soldering iron was used to heat the outer wall of the sample tube around the deposited frozen gas while the bottom of the sample test tube was submerged in the liquid nitrogen bath. The remaining gas in the system was cryo-pumped back into the gas tank. The completed sample tube was then transferred to the pre-cooled probe as quickly as possible (within at most a few minutes).

A summary of the pressures and temperatures of the target gases is displayed in Table 1.

DNP System

The DNP/NMR system consisted of a 5T Oxford TMR7/88/15 TeslatronMR shielded magnet with an integrated, internally filled, externally pumped ^{4}He cryostat. The pumping system reached a base temperature of 1.35 K and was monitored by four LakeShore cernox CX-1030-SD sensors. The sensors were probed using using a RV-Elektronikka AVS-47 resistance bridge (0.2% resolution) and were located at three different elevations (~10, 20 and 30 mm) above the microwave chamber to allow precise detection of liquid helium level during microwave irradiation. Microwave power was generated by a co-controlled primary narrowband microwave source at 7.8 GHz, 18.3 dBm (Hewlett- Packard 83623B). This was followed by a set of removable attenuators to adjust the final output power and thereby control sample heating during DNP. The microwave frequency was increased to 140 GHz by a ×18 frequency multiplier and a narrowband 140 GHz, 70mW microwave amplifier (ELVA DCOIMA-06/140/70) mounted on the custom-made probe, as shown in Figure 3. The microwave radiation was transmitted through a 3/16” stainless steel overmoded circular waveguide into a 50 mm aluminum microwave chamber mounted on the probe.

The top section of the probe has a 50-mm vacuum port and sample insertion/retrieval port. Samples can be inserted into the chamber in either 5mm tubes or in a custom-made 3-inch-long sample cup with an effective volume of 2 ml similar to that of the HyperSense commercial DNP instrument (Figure 3). The latter setup provided direct contact between the sample and the liquid helium, thus reducing the sample’s internal temperature. This port was connected to the microwave chamber using a long G10 fiber-plastic tube, providing a direct sample insertion and extraction route. This tube opened to a perforated G10 sleeve of the same diameter mounted on a sample pedestal at the bottom of the sample chamber. The perforation on this tube provided additional helium flow into the sample for more efficient cooling. A 15-mm two-turn insulated copper saddle NMR coil was wrapped around the perforated G10 tube in the sample chamber to acquire NMR spectra.

A home-built spectrometer was used to record the NMR spectra with small flip angle pulses (2-6°). The repetition time between excitations was no shorter than 20 minutes. After applying baseline adjustment, FFT, and up to first-order phase correction, spectra were fitted to single or multi-Gaussian line shapes unless otherwise specified. The individual peak

integrals were computed from Gaussian fitting (for ^{129}Xe) or directly by numerical integration (for $^{15}N_2O$) of the peaks. The reported areas and widths were corrected for the effects of a 9.5-μs digitizer dead time. Polarization for ^{129}Xe species was calculated by normalizing the peak integrals (obtained from the fit parameters) to the corresponding thermally relaxed values measured from the same sample without DNP at the base temperature of the cryostat and using the theoretical Boltzmann polarization value of a spin-½ system, $P_{½} = \tan h\,(hf/2kT)$, where h and k are respectively the Planck and Boltzmann constants, f is the NMR frequency, and T is the temperature. The $^{15}N_2O$ polarization was not measured due to extremely long T_1 relaxation times; however, the signal intensities were compared given the sample volume and experimental conditions.

To optimize conditions during DNP, an experiment was conducted to monitor polarization buildup while adjusting the flow of liquid helium from the magnet reservoir into the cryostat. Initially, the cryostat was filled with liquid helium internally while the pump port was fully open, until the superfluid helium level at 1.65K rose above the third sensor (Figure 3). At that point, the fill was stopped by closing the needle valve connecting the cryostat to the main helium reservoir of the magnet, at which point the vacuum pump cooled the system down to 1.42K. We refer to this method as “helium overfilling”.

Methods for increasing polarization level

In addition to refining the gas mixing and DNP processes, we experimented with two other techniques for optimizing the polarized sample. Pulverization is a process in which the solid sample is crushed into smaller pellets, drastically increasing the surface area of the sample and making the process of polarization more efficient. In annealing, the temperature of the sample is transiently increased from liquid helium temperature to a much higher temperature, thereby allowing freer diffusion of atoms and leading to segregation of the mixture components on a microscopic scale.

Pulverization—Xenon sample I (homogeneously mixed) was polarized at 1.42K in the 5 mm NMR tube and then removed from the spectrometer under liquid nitrogen. It was transferred to the bottom of a Styrofoam box containing approximately 2 cm of liquid nitrogen. While still under the liquid nitrogen, the sample was carefully pulverized with a precooled plier into 10-12 frozen pellets with 2-3mm diameter, after which it was transferred into the custom-built PEEK sample cup. The sample was then quickly reinserted into the NMR/DNP probe under liquid nitrogen. The coil temperature was maintained between 85 and 100K in order to ensure full evaporation of any liquid nitrogen that might be remaining in the sample cup prior to cooling. The sample was subsequently polarized at 1.42K.

Annealing—Xenon sample II, which was initially homogenously mixed, was annealed inside the NMR magnet for 20 hours at 125K after initial DNP characterization. The insert hosting the 5mm sample tube was warmed using the built-in heater, and the temperature was monitored using the temperature sensors. A different approach was used for the $^{15}N_2O$ sample based broadly on the approach established in (11); annealing was performed as an additional step in sample preparation. After mixing, the sample was transferred to the annealing bath outside of the magnet for approximately an hour and was returned to the

magnet for re-characterization. The process was repeated twice, and the sample was characterized after each annealing. Different baths were used for each step. Initial annealing was performed at 154±2K for 65 minutes by inserting the 5mm sample tube containing the sample into a glass dewar containing using an ethanol/ethanol ice bath. The sample was then placed in the probe and polarized at 1.42 K. The second annealing was performed outside the magnet for 65 minutes in a similar manner using a toluene/toluene ice bath at 180±2K. Figure 7.A depicts the recorded temperature of both baths over time measured using a resistance temperature detector (RTD) with 0.2% resolution.

RESULTS

By taking advantage of the three sensors used in the construction of our DNP system, we were able to demonstrate the effect of sample temperature on the level of polarization of the xenon sample. Figure 4 demonstrates the increase in signal buildup at two temperatures: 1.65K and 1.42K. The signal buildup for these temperatures was assessed consecutively, first at 1.65K using helium overfilling, and then at 1.42K by closing the needle valve after the helium overfilling and thereby allowing the temperature to drop. This maneuver resulted in a small change in temperature but led to an increase of >15% in signal buildup. The helium overfilling technique thus noticeably improved sample polarization level.

To further increase the polarization of the target samples, we investigated the effect of pulverization. Figure 5 shows polarization build-up curves for xenon sample I before and after crushing. The data suggest a slight increase in the spin-up time constant (T_B) from 131 ± 28 min (dots) to 161 ± 30 min upon pulverizing (circles). Further comparison between the polarization build-up curves indicates an increase in polarization by a factor of ~2 due to increased contact area between liquid helium and the pellets, resulting in more efficient circulation of liquid helium around the pellets. Maximum polarizations of 10±1% and 20±3% were achieved for the intact and the pulverized samples, respectively.

Annealing was also tested to assess its ability to enhance the polarization properties of gas samples. We found that the annealing process impacts both the lineshape of the spectra and T_1 relaxation times—the two major factors in a compound's level of polarization. Figures 6.A and 6.B show the low-temperature DNP ^{129}Xe spectra before and after annealing of the sample. The single broad peak in Figure 6.A represents a homogenous Xe/1-propanol/ radical matrix. Figure 6.B demonstrates that the annealing process (maintaining 125K for 20 hours) resulted in a distinct peak with linewidth and chemical shift consistent with clusters of pure ^{129}Xe ice (solid line). The annealing also reduced the line width and decreased the chemical shift of the broad peak. Figures 6.C and 6.D show a substantial increase in T_1 relaxation time after annealing. Relaxation time was T_1=212 ± 3 minutes before annealing. Annealing the sample resulted in 708±17 minutes for the broad peak (homogenous part of the sample) and 2087±45 minutes for the narrow peak (xenon clusters).

We performed a series of studies using progressive annealing of $^{15}N_2O$ at two temperatures, as shown in Figure 7.A (dashed line for ethanol/ethanol ice, solid line for toluene/toluene). Figure 7.B depicts a direct comparison of the spectra of the $^{15}N_2O$ sample after each period of annealing. Figure 7.C displays a direct comparison between the area under the peaks

during DNP after short and long annealing times; long annealing resulted in a ~2-fold increase in the total signal intensity. The absolute polarization in this case was not measured due to the extremely long T_1 (several tens of hours).

DISCUSSION

While optical pumping is a well-established approach for polarizing noble gases, a shift to the use of DNP for HP gas MRI would present a number of advantages. DNP technology is rapidly being adopted on a global scale, making it significantly more accessible than optical pumping; it has the capability to polarize molecular gases, which would diversify the field of HP gas imaging; and it has the potential to eventually generate gases with higher polarization and greater volume than that achieved by optical pumping. As part of the early effort to test the feasibility of a shift to gas DNP, the studies described here tested a series of techniques designed to improve the DNP characteristics of gaseous targets. The strategies employed resulted in significant improvements to solid-state polarization for both gases and T_1 relaxation time for the ^{129}Xe gas. Similar results have been reported in our earlier work on $^{15}N_2O$ (11).

The sample production apparatus described above allows for tight control of the temperature and pressure of ^{129}Xe- and $^{15}N_2O$-based samples. Successful DNP requires homogenous mixtures of target molecule and radical (4,11,12). While producing such samples is straightforward for ^{13}C substrates, it is much more challenging to create well-mixed DNP samples with gaseous targets, as the target gas and radical/glassing agent have to be in liquid phase at the same time. Accurate measurement of temperature and pressure is crucial to controlling the phase of sample constituents. In contrast to our older system (4,11), the new manifold directly measures gas volume and pressure, making the regulation of sample composition far easier. This resulted in homogeneously mixed samples, as evidenced by the single-peak lineshape of the ^{129}Xe mixture shown in Figure 6.A; in our past studies (4,18), samples that were not well mixed generated spectra with two distinct peaks separately reflecting the pure ^{129}Xe and the glassy matrix.

For any DNP sample, achieving a high polarization requires an efficient polarizer. Because polarization increases at larger B_0 (at least within the region of easily accessible field strengths), our home-build DNP system at 5T produces samples with higher polarization than is readily achieved in the HyperSense commercial polarizer at 3.35T (3,7). The new probe in our home-built DNP system allows for direct, accurate determination and control of the lattice temperature using multiple temperature sensors. Reducing the temperature of the sample during DNP is another key factor for increasing polarization (13). The increase in signal after reducing the temperature from 1.65K to 1.42K using the helium overfilling technique (seen in Figure 4) reflects the sample's advantageous response to a reduced heat load in the overfull insert when the microwave source is turned on. Further decreases in temperature in our system could be achieved by using a more efficient vacuum pump, which would reduce the base temperature of the system below the current 1.35K (15).

Although the base temperature of the system is a limiting factor, previous work on ^{129}Xe (4) showed that sample overheating can occur for samples in the NMR tube since it acts as a

thermal barrier between the sample and the liquid helium during microwave irradiation. Gas DNP can be enhanced by increasing the contact area between the solid sample and liquid helium; pulverizing the original ^{129}Xe sample in the 5mm tube (120 mL) to 10-12 pellets, 2-3 millimeter in size, increases to surface to volume ration by ~2. This process therefore mitigates sample overheating during microwave irradiation both by increasing sample surface-to-volume ratio and removing the glass thermal barrier.

When applying this technique, rapid transfer of the sample into the DNP system after pulverization is essential to prevent gas loss via sublimation. Here, we have improved pulverization and transport methods from our previous study (4) to quickly and efficiently produce highly polarized solid ^{129}Xe. Using the custom-made PEEK sample cup in conjunction with a simplified sample insertion technique through a port on the top of the NMR/DNP probe (Figure 3), we inserted the pulverized sample into the pre-cooled probe in a few seconds. The resulting two-fold gain in polarization using this technique is demonstrated in Figure 5.

While it is imperative to have homogenously mixed samples to achieve efficient polarization during DNP (12), our previous studies (4,11) demonstrated that the T_1 relaxation time of hyperpolarized ^{129}Xe in DNP experiments is a strong function of the thermal history of the sample. Annealing the sample at higher temperatures (above 120K) partially segregates pure xenon species from the matrix as a result of atomic diffusion. Consequently, the mixture undergoes a glass transition at higher temperatures over a long time period. This effect can increase the T_1 relaxation constant and subtle changes in the NMR lineshape indicate the formation of domains of sample inhomogeneity. Better sample mixing typically results in a broader and symmetric solid NMR spectrum (Figure 6.A) due to dipolar coupling between target nuclei and ^{1}H magnetic moments of uniformly distributed 1-propanol molecules. On the other hand, less broadening in the solid-state NMR spectrum and a slight change in chemical shift (Figure 6.C) after annealing indicates reduced or insignificant coupling to the protons in the sample. In the case of ^{129}Xe, the changes in line width and frequency are consistent with the known values of 1-propanol-induced broadening and chemical shift of ^{129}Xe (4). However, unlike samples that were initially poorly mixed, the pure ^{129}Xe peaks of annealed samples respond to DNP. This indicates a much smaller pure ^{129}Xe domain for which interaction with the radical (either direct or by spin diffusion) is sufficient for substantial polarization of the interior atoms. Based on our previous study (4,18), annealing does not increase the overall polarization of xenon during DNP. However, the remarkable increase in T_1 relaxation time constant as demonstrated in Figure 6 can facilitate transport of polarized samples to MRI sites for imaging.

In the case of $^{15}N_2O$, annealing was included by default as an additional step in sample preparation. Previous investigations on the DNP of inhomogeneous $^{15}N_2O$ had demonstrated segregation of $^{15}N_2O$ molecules similar to that observed in ^{129}Xe, but leading to an increase in polarization by a factor of ~2 and an increase in T_1 from 8 hours to 33 hours at 1.42K (11). Here, we also examined the effect of progressive annealing of $^{15}N_2O$ over two steps, as demonstrated in Figure 7. Our results show that the annealing is significantly more effective at ~180K, leading to a 2-fold increase in signal. This gain is also observed in (11) wherein we annealed a well-mixed sample at a similar temperature, increasing the polarization from

~5% to ~10%. The distinct quadruplet of powder-pattern spectra—a characteristic signature of two different chemical shift anisotropy (CSA) tensors further split by the direct dipole-dipole interaction between the neighboring ^{15}N spins—becomes visible later in the DNP process. This pattern becomes more pronounced after the second annealing as in (11) due to more rapid segregation of the ^{15}N nuclei achieved at higher temperature. Note that in both cases, the gradual sharpening of the powder-pattern features over time during DNP suggests growth of the pure $^{15}N_2O$ magnetization relative to that of homogenous matrix $^{15}N_2O$. We note that CSA in the N_2O molecule is still present in the domains of pure N_2O, but no analogous effect is present in the annealed ^{129}Xe domains. This may affect spin diffusion across the domain boundary and account for the differing results with the two gases.

CONCLUSION

We have presented a set of new techniques for producing and manipulating solid gas/glassing agent/radical mixtures for DNP. Several aspects of our approach were shown to enhance the polarization and T_1 relaxation time. The reduction of the ^{129}Xe sample temperature during DNP and pulverization of the sample increases polarization. Since the same mechanisms are involved, we expect that pulverization will similarly increase $^{15}N_2O$ polarization. Controlled annealing of a well-mixed ^{129}Xe sample was shown to substantially increase solid T_1, and it increased polarization in $^{15}N_2O$. Annealing has been previously shown to increase T_1 in the case of $^{15}N_2O$ as well (11). While optical pumping can generate large quantities of highly polarized xenon, the methods introduced in this study demonstrate the feasibility of using DNP—a more widely accessible technology—for effectively polarizing xenon as well as other gases that are not polarizable via optical pumping.

Acknowledgments

This work was supported by the National of Institutes of Health (NIH) R01 EB015767.

References

1. Fain SB, Korosec FR, Holmes JH, O'Halloran R, Sorkness RL, Grist TM. Functional lung imaging using hyperpolarized gas MRI. J Magn Reson Imaging. 2007; 25:910–923. DOI: 10.1002/jmri.20876 [PubMed: 17410561]
2. Matsuoka S, Patz S, Albert MS, Sun Y, Rizi RR, Gefter WB, Hatabu H. Hyperpolarized Gas MR Imaging of the Lung: Current Status as a Research Tool. Journal of Thoracic Imaging. 2009; 24:181–188. DOI: 10.1097/RTI.0b013e3181b32bec [PubMed: 19704321]
3. Comment A, Comment A, Jannin S, et al. Hyperpolarizing Gases via Dynamic Nuclear Polarization and Sublimation. Phys Rev Lett. 2010; 105 Internet. doi: 10.1103/PhysRevLett.105.018104
4. Kuzma NN, Pourfathi M, Kara H, Manasseh P, Ghosh RK, Ardenkjaer-Larsen JH, Kadlecek SJ, Rizi RR. Cluster formation restricts dynamic nuclear polarization of xenon in solid mixtures. J Chem Phys. 2012; 137:104508–6. DOI: 10.1063/1.4751021 [PubMed: 22979875]
5. Capozzi A, Roussel C, Comment A, Hyacinthe J-N. Optimal Glass-Forming Solvent Brings Sublimation Dynamic Nuclear Polarization to 129Xe Hyperpolarization Biomedical Imaging Standards. J Phys Chem C. 2015; 150213150722008. doi: 10.1021/jp5124053
6. Ardenkjaer-Larsen, JH.; Hansson, L. Method for the production of hyperpolarized 129Xe. Patent No US. 20060173282 A12011.
7. Jannin S, Comment A, Kurdzesau F, Konter JA, Hautle P, van den Brandt B, van der Klink JJ. A 140 GHz prepolarizer for dissolution dynamic nuclear polarization. J Chem Phys. 2008; 128:241102.doi: 10.1063/1.2951994 [PubMed: 18601309]

8. Hersman FW, Ruset IC, Ketel S, et al. Large Production System for Hyperpolarized 129Xe for Human Lung Imaging Studies. Acad Radiol. 2008; 15:683–692. DOI: 10.1016/j.acra.2007.09.020 [PubMed: 18486005]
9. Happer W, Miron E, Schaefer S, Schreiber D, van Wijngaarden W, Zeng X. Polarization of the nuclear spins of noble-gas atoms by spin exchange with optically pumped alkali-metal atoms. Phys Rev A. 1984; 29:3092–3110. DOI: 10.1103/PhysRevA.29.3092
10. Cleveland, ZI.; Cofer, GP.; Metz, G., et al. Hyperpolarized 129Xe MR Imaging of Alveolar Gas Uptake in Humans. In: Yang, S., editor. PLoS ONE. Vol. 5. 2010. p. e12192
11. Kuzma NN, Håkansson P, Pourfathi M, Ghosh RK, Kara H, Kadlecek SJ, Pileio G, Levitt MH, Rizi RR. Lineshape-based polarimetry of dynamically-polarized 15N2O in solid-state mixtures. Journal of Magnetic Resonance. 2013; doi: 10.1016/j.jmr.2013.06.008
12. Ardenkjaer-Larsen JH. Increase in signal-to-noise ratio of > 10,000 times in liquid-state NMR. Proceedings of the National Academy of Sciences. 2003; 100:10158–10163. DOI: 10.1073/pnas.1733835100
13. Lumata L, Kovacs Z, Sherry AD, Malloy C, Hill S, van Tol J, Yu L, Song L, Merritt ME. Electron spin resonance studies of trityl OX063 at a concentration optimal for DNP. Phys Chem Chem Phys. 2013; 15:9800–9807. DOI: 10.1039/c3cp50186h [PubMed: 23676994]
14. Meyer W, Heckmann J, Hess C, Radtke E, Reicherz G, Triebwasser L, Wang L. Dynamic polarization of13C nuclei in solid13C labeled pyruvic acid. Nucl Instrum Methods Phys Res A. 2011; 631:1–5.
15. Jóhannesson H, Macholl S, Ardenkjaer-Larsen JH. Dynamic Nuclear Polarization of [1-13C]pyruvic acid at 4.6 tesla. Journal of Magnetic Resonance. 2009; 197:167–175. DOI: 10.1016/j.jmr.2008.12.016 [PubMed: 19162518]
16. Hovav Y, Feintuch A, Vega S. Theoretical aspects of dynamic nuclear polarization in the solid state-The solid effect. Journal of Magnetic Resonance. 2010; 207:176–189. DOI: 10.1016/j.jmr.2010.10.016 [PubMed: 21084205]
17. Lee Y, Zacharias NM, Piwnica-Worms D, Bhattacharya PK. Chemical Reaction-Induced Multi-molecular Polarization (CRIMP). Chem Commun. 2014; 50:13030–13033. DOI: 10.1039/C4CC06199C
18. Pourfathi M, Kuzma NN, Kara H, Ghosh RK, Shaghaghi H, Kadlecek SJ, Rizi RR. Propagation of dynamic nuclear polarization across the xenon cluster boundaries: Elucidation of the spin-diffusion bottleneck. Journal of Magnetic Resonance. 2013; 235:71–76. DOI: 10.1016/j.jmr.2013.07.006 [PubMed: 23981341]
19. Mugler JP, Altes TA. Hyperpolarized 129Xe MRI of the human lung. J Magn Reson Imaging. 2013; 37:313–331. [PubMed: 23355432]
20. Chang YV, Quirk JD, Ruset IC, Atkinson JJ, Hersman FW, Woods JC. Quantification of human lung structure and physiology using hyperpolarized 129Xe. Magn Reson Med. 2013; 71:339–344. DOI: 10.1002/mrm.24992 [PubMed: 24155277]
21. Marco-Rius I, Tayler MCD, Kettunen MI, et al. Hyperpolarized singlet lifetimes of pyruvate in human blood and in the mouse - Marco-Rius - 2013 - NMR in Biomedicine - Wiley Online Library. NMR Biomed. 2013; 26:1696–1704. Internet. DOI: 10.1002/nbm.3005 [PubMed: 23946252]
22. K GR, Kadlecek SJ, Kuzma NN, Rizi RR. Determination of the singlet state lifetime of dissolved nitrous oxide from high field relaxation measurements. J Chem Phys. 2012; 136:174508.doi: 10.1063/1.4710984 [PubMed: 22583250]
23. Ghosh RK, Kadlecek SJ, Ardenkjaer-Larsen JH, Pullinger BM, Pileio G, Levitt MH, Kuzma NN, Rizi RR. Measurements of the persistent singlet state of N2O in blood and other solvents-Potential as a magnetic tracer. Magn Reson Med. 2011; 66:1177–1180. DOI: 10.1002/mrm.23119 [PubMed: 21928358]
24. Pileio G, Carravetta M, Levitt MH. Storage of nuclear magnetization as long-lived singlet order in low magnetic field. pnas org.
25. Matta, BF.; Menon, DK.; Smith, M. Core Topics in Neuroanaesthesia and Neurointensive Care. Cambridge University Press; 2011.

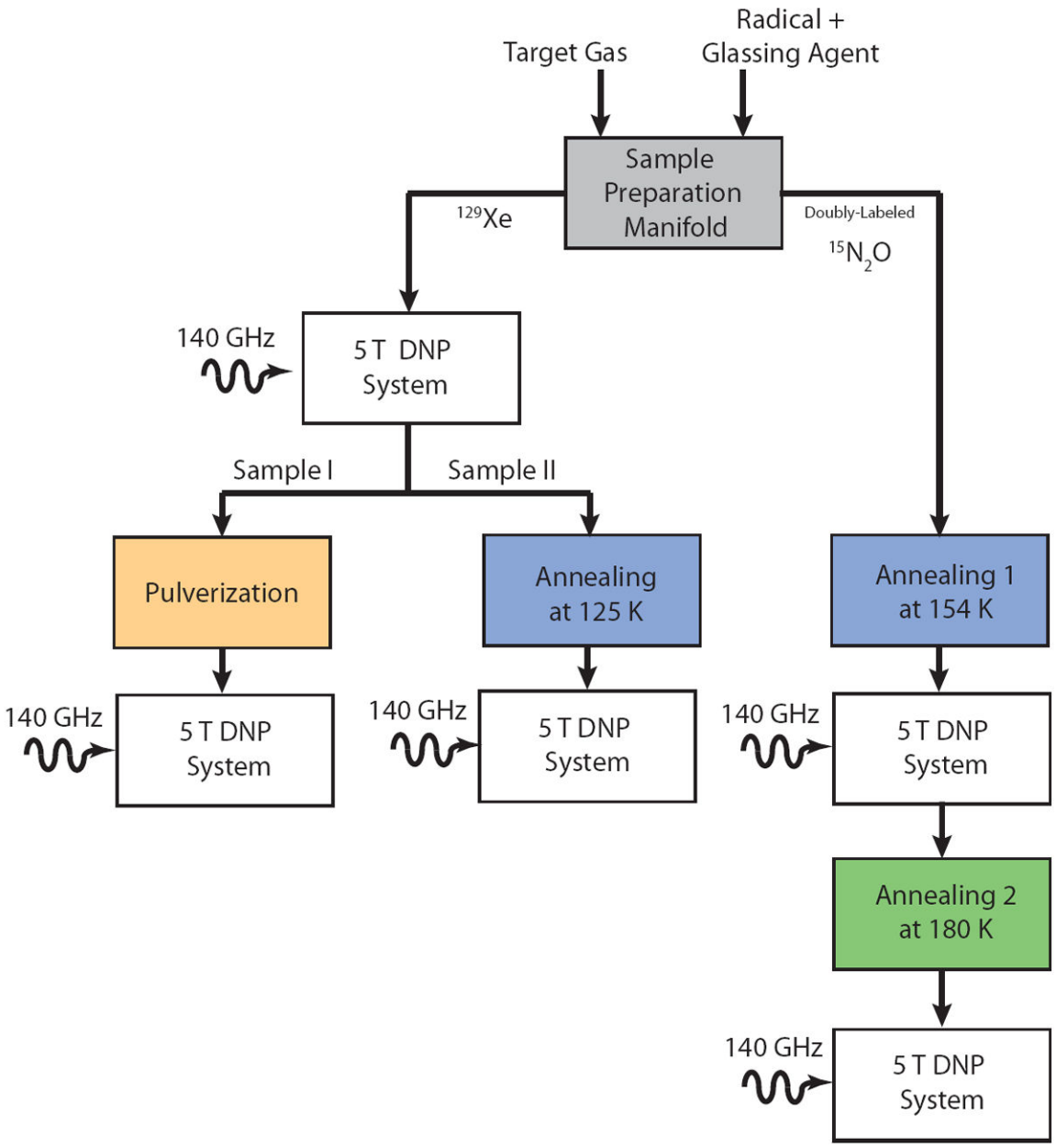

Figure 1.
Schematic representation of the experiments

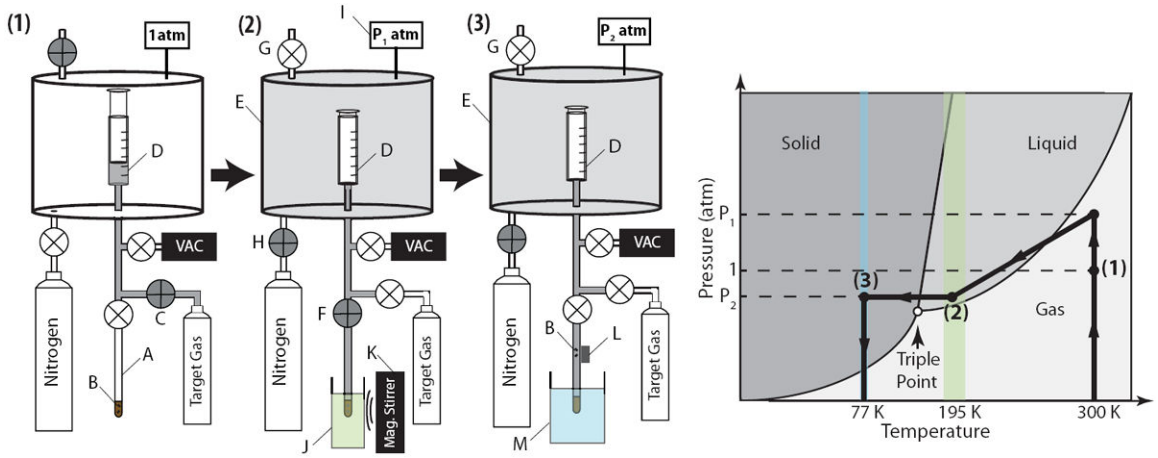

Figure 2.

Images 1-3 depict the steps to prepare the gaseous sample. A. 5-mm NMR tube containing 1-propanol-radical mixture B. Small magnetic stir bars C. Pure gas tank valve D. Glass syringe E. Sealed pressure vessel F. Sample tube valve G. Vessel pressure release valve H. Nitrogen/Air gas valve for pressurizing the vessel I. Pressure Gauge J. Liquefaction bath (ethanol/dry ice) K. Magnetic stirrer L. Small permanent magnet to retrieve the stir bars M. Liquid nitrogen bath. The panel on the right shows the phase trajectory on the phase diagram during the sample preparation.

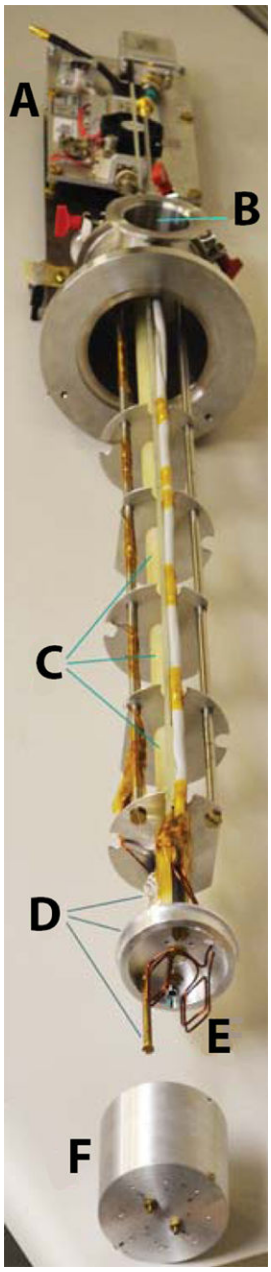

Figure 3.

Our home-built DNP insert: **A.** 140 GHz microwave source. **B.** 50-mm vacuum port. **C.** Perforated G10 tube **D.** Three temperature sensors installed at different elevations **E.** Two-turn saddle 15 mm coil mounted around the G10 tube. **F.** Microwave chamber.

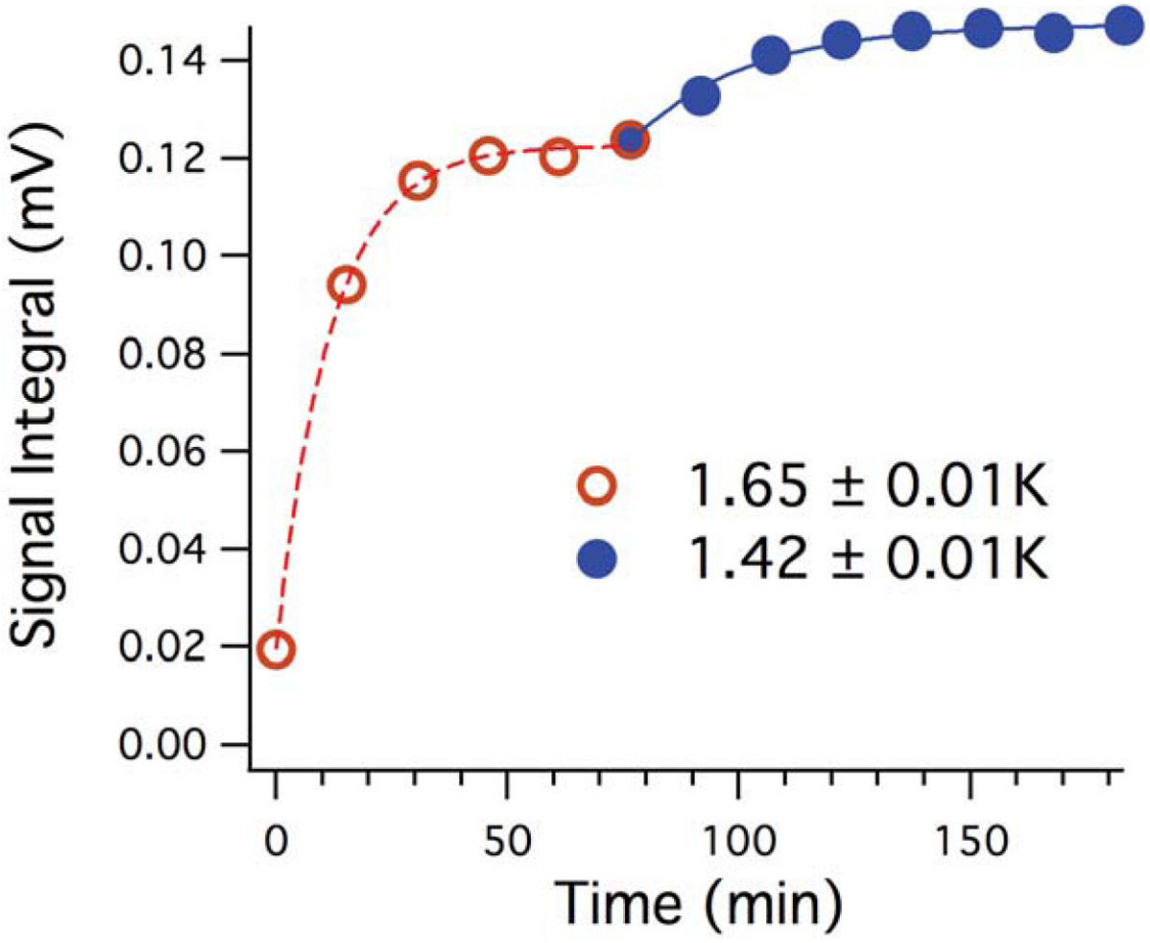

Figure 4.
Influence of temperature on enhancement during polarization of ^{129}Xe. Temperature measurement is from the bottom sensor closest to the insert.

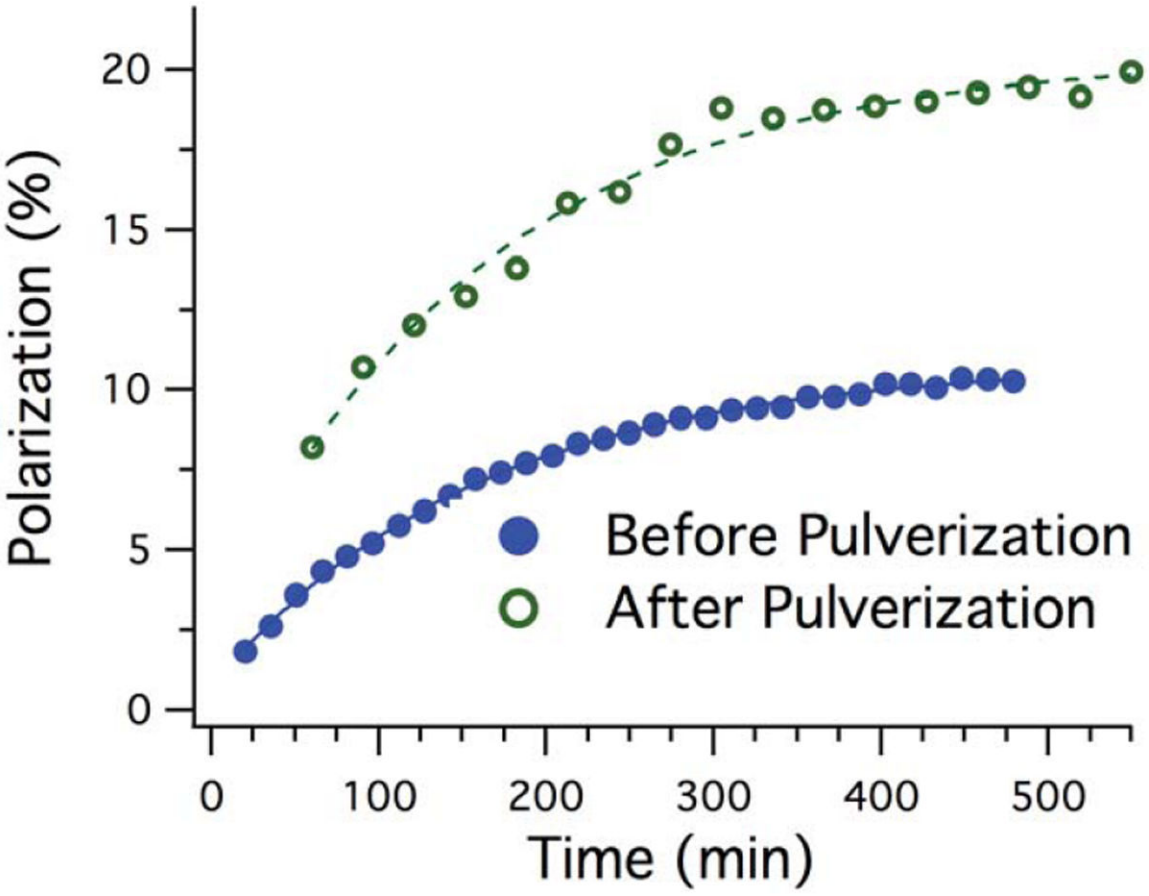

Figure 5.
Polarization build-up of the solid xenon mixture before (open circles) and after (filled circles) pulverization.

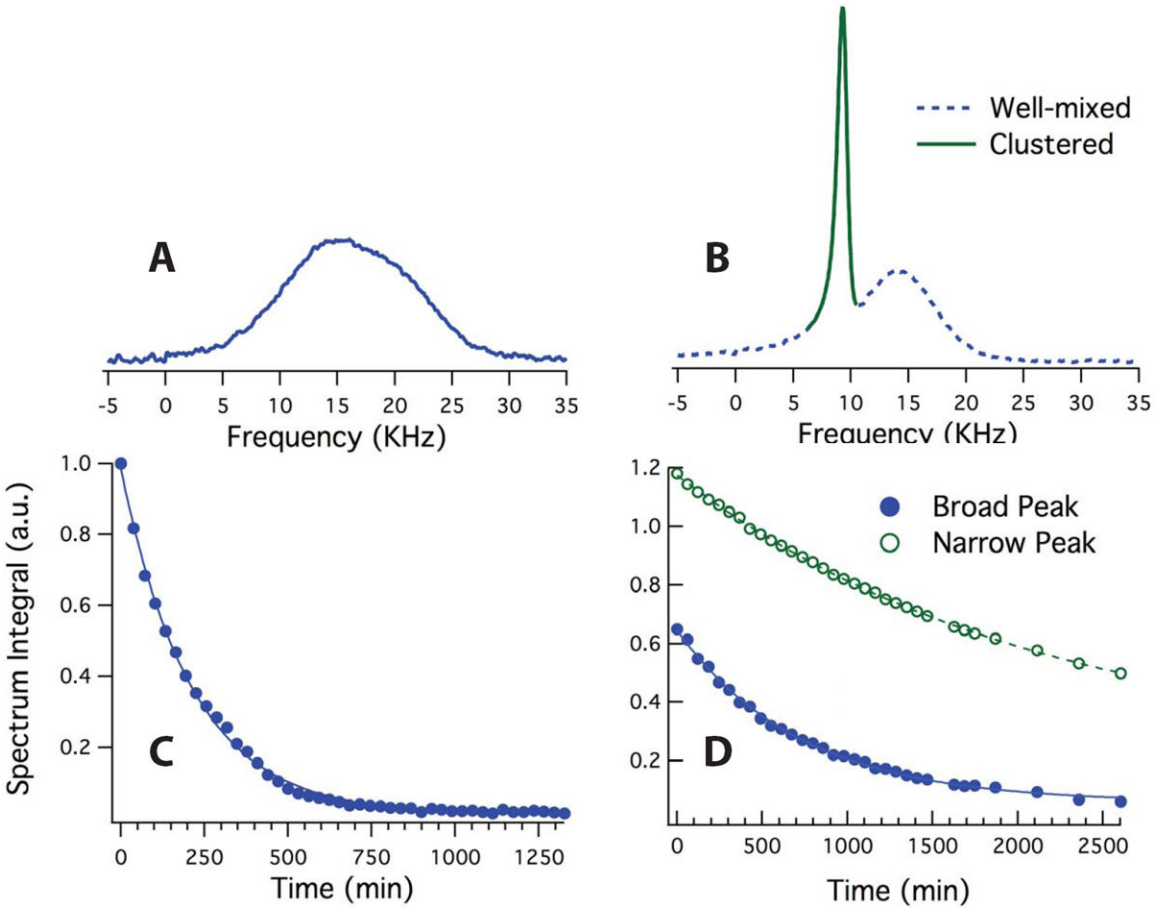

Figure 6.

^{129}Xe NMR spectra and area under the peaks acquired from sample II after 9 hours of DNP at 1.42K before **(A,C)** and after **(B,D)** controlled annealing. **(C)** shows the area under the peak in **(A)** during relaxation. The solid line is the exponential fit to the data indicating a T_1 of 212±3 minutes. **(D)** shows the area under the broad (filled circles) and narrow (open circles) peaks during relaxation. The exponential fits yield T_1 relaxation times of 708±17 minutes and 2087±45 minutes for the broad and narrow peaks, respectively.

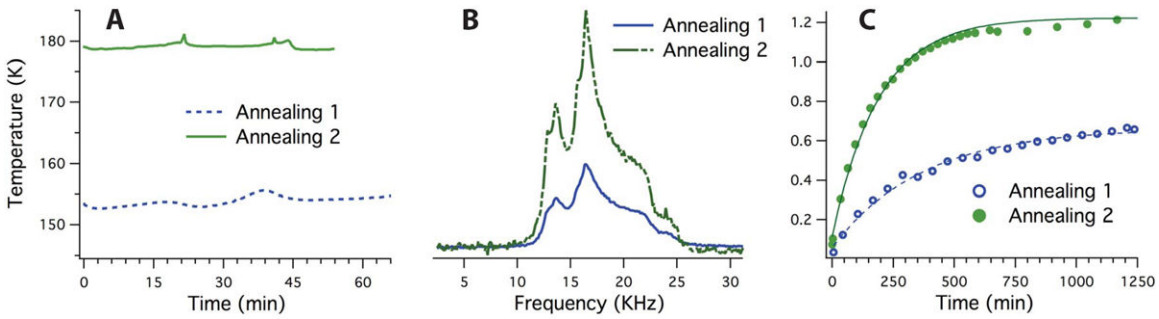

Figure 7.

(A) Temperatures of ethanol/ethanol ice (dashed line) and toluene/toluene ice (solid line) baths measured during controlled annealing. The temperatures were stabilized to be within ±2 K of the target annealing temperatures. (B) Comparison of $^{15}N_2O$ spectra after ~20 hours of DNP and (C) polarization build-up after short (annealing 1) and after long (annealing 2) controlled annealing at ~154 K and ~180 K, respectively. Note the significant increase in the signal intensity after the longer annealing.

TABLE 1

Physical Properties of the target gases and conditions during sample preparation

	1 atm pressure		Triple Point		Sample Preparation		
Gas	**T_{melt} (K)**	**T_{boil} (K)**	**T (K)**	**P (atm)**	**T (K)**	**P (atm)**	**Bath**
^{129}Xe	161.04	165.62	161.3	0.804	195	4.2	Ethanol/Dry Ice
$^{15}N_2O$	182.29	184.67	182.34	0.866	195	1.75	Ethanol/Dry Ice